Attitude Parameter Inspired Relative Motion Descriptions for Relative Orbital Motion Control

Erik A. Hogan* and Hanspeter Schaub†
University of Colorado at Boulder, Boulder, Colorado 80309

DOI: 10.2514/1.60626

This paper describes the development of novel relative orbital motion descriptions for a two craft formation, defined by a separation distance and relative orientation parameter set. These descriptions allow for the use of separation distance as a state parameter for the relative motion, while avoiding singularity issues that plague spherical coordinate descriptions. Instead, Euler parameterlike or modified Rodrigues parameterlike coordinates are employed to describe the relative orientation. Equations of motion are developed that allow propagation of these new descriptions for the case of a circular reference orbit and small separation distances between the craft. These equations of motion are derived from the Clohessy–Wiltshire equations. Feedback control laws are developed to stabilize the relative motion between the craft. Numerical simulation is used to compare the newly developed relative motion descriptions with inertial equations of motion. The results validate these new descriptions as a practical method for describing relative motion.

I. Introduction

IN RELATIVE motion studies of spacecraft formations, the Hill-frame coordinates are a commonly used relative position and velocity description between a chief craft and a deputy craft. These coordinates are a Cartesian description, and applying them to the special case of a circular chief orbit with small separation distances results in the Clohessy–Wiltshire (CW) equations [1]. For some applications, a curvilinear coordinate frame is preferred and used to describe the relative motion; this curvilinear coordinate frame is typically a spherical frame, defined by the separation distance between the craft and two angles that provide information about the orientation of the line of sight vector from the chief to the deputy [2]. Another relative motion description uses differential orbital elements [3]. Here, one craft in the formation is specified as the reference craft, and all other craft in the formation are defined by differencing their orbital elements with those of the reference. The relative motion problem has also been parameterized and studied using a quaternion formulation [4].

In the current study, motion with respect to a circular chief orbit will be investigated using an alternative relative position description. In some cases, relative motion descriptions that use the separation distance between the chief and deputy as a coordinate are sought. This can be important for certain applications in which the separation distance has a direct impact on the dynamics and control of the formation or in which collision is a real possibility. One such application in which these concerns are applicable is found in [5]. Here, electrostatic forces are used to generate a contactless tugging force between the chief and deputy, allowing the chief to thrust and tow the deputy into a new orbit [6,7]. Further, the ion-beam shepherd method for large debris removal also requires close proximity flying on the order of dozens of meters, in which the separation distance errors should be controlled more strongly than the relative heading errors [8–10]. To develop the relative motion control law, spherical coordinates are chosen because the separation distance appears directly in the electrostatic force expression. Thus, it is advantageous for the distance between the deputy and chief to appear as a state in the relative equations of motion. Furthermore, spherical coordinates provide a simple way to prescribe relative trajectories in which the chief maneuvers around the deputy while maintaing a safe separation distance, as only the angles need modification during the maneuver. Using a spherical coordinate system to describe the relative motion results in kinematic singularities, however; it is of interest to study other potential relative position descriptions that may avoid these issues. By deriving the relative motion using alternate descriptions, new dynamical equations that have potentially advantageous properties are obtained.

When using spherical coordinates, kinematic singularities may appear, depending on how the angles are defined. For example, in [2], no singularities are encountered because the spherical frame is defined relative to an inertial frame, and the equations are linearized. In [5], however, the spherical frame is defined relative to the rotating Hill frame, and kinematic singularities result because arbitrary relative motion is considered. The singularities arise when the deputy is directly above or below the chief in the orbit normal direction. Clearly, this eliminates a wide range of trajectories from consideration when using spherical coordinates. Further, because this orbit normal relative position is a singular configuration, the previously developed control in [5] would not be able to perform orbital plane change maneuvers using the electrostatic tug. In spite of these singularities, the spherical frame is used because it contains the separation distance as a state.

In the current study, alternate relative motion descriptions are sought, which use the separation distance as a state but avoid the singularities associated with using spherical coordinates. To that end, one relative position description, inspired by the Euler parameter attitude set, is proposed, which uses a once-redundant set of parameters to describe the relative orientation of the craft in the formation. The relative orientation is parameterized using the components of the unit vector, which points from the chief to the deputy. Beyond this unit-vector description, a relative motion description is constructed that contains two possible sets of parameters for describing the relative orientation in conjunction with the separation distance. While these two possible sets contain singularities, these singularities do not occur at the same relative orientation, very similarly to the behavior of the modified Rodrigues parameter attitude description [11–14]. Thus, a switching condition may be employed to avoid these singularities altogether. Beyond developing and analyzing the corresponding equations of motion for these new relative motion descriptions, control laws employing continuous feedback are derived to stabilize the relative motion.

The paper is structured as follows. First, background information regarding relative orbital motion is provided, including the

Presented as Paper 2012-4379 at the AAS/AIAA Astrodynamics Specialist Conference, Minneapolis, MN, 13–16 August 2012; received 5 October 2012; revision received 23 September 2013; accepted for publication 23 September 2013; published online 26 March 2014.

*Graduate Student.
†Associate Professor, Aerospace Engineering Sciences.

Clohessy–Wiltshire equations. Then, the unit-vector description is introduced, and its equations of motion are derived. Next, the $\boldsymbol{\sigma}$ set is defined, and its corresponding dynamical equations are obtained. Control laws for reference trajectory tracking are developed, and numerical simulation is used to illustrate their performance.

II. Relative Orbit Descriptions Using Heading and Separation Distance Measures

A. Clohessy–Wiltshire Equations

In this paper, the relative motion of a deputy satellite with respect to a chief is studied. This scenario is depicted in Fig. 1. Here, $\boldsymbol{r}_c$ describes the inertial position of the chief, and $\boldsymbol{r}_d$ describes the position of the deputy. The relative position $\boldsymbol{\rho}$ is defined as

$$\boldsymbol{\rho} = \boldsymbol{r}_d - \boldsymbol{r}_c \tag{1}$$

Of interest is how this relative position evolves under the influence of natural orbital motion and a deputy control input. One relative motion description frequently used is the Cartesian Hill-frame coordinate system, illustrated in Fig. 1. The axes of the Hill frame are computed using

$$\hat{o}_r = \frac{\boldsymbol{r}}{r}, \qquad \hat{o}_\theta = \hat{o}_h \times \hat{o}_r, \qquad \hat{o}_h = \frac{\boldsymbol{r} \times \dot{\boldsymbol{r}}}{|\boldsymbol{r} \times \dot{\boldsymbol{r}}|} \tag{2}$$

In this study, two assumptions are made. The first is that the separation distance between the chief and deputy is much smaller than their respective orbit radii. Second, it is assumed that the chief is on a circular orbit with a constant mean motion n. Under these assumptions, the relative equations of motion may be simplified to the well-known CW equations [1],

$$\ddot{x} - 2n\dot{y} - 3n^2 x = u_x \tag{3a}$$

$$\ddot{y} + 2n\dot{x} = u_y \tag{3b}$$

$$\ddot{z} + n^2 z = u_z \tag{3c}$$

where x,y, and z are Hill-frame components of the relative position vector $\boldsymbol{\rho}$ and u_x, u_y, and u_z are control accelerations in the x, y, and z directions, respectively. The CW equations will be used to derive the equations of motion for the following novel relative motion descriptions.

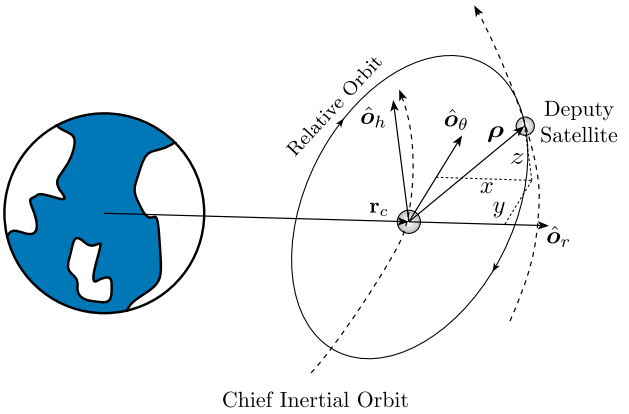

Fig. 1 Relative motion of the deputy and chief, illustrated using a rotating Hill frame.

B. Unit-Vector Description

It is sometimes of interest to use the separation distance between the craft directly as a coordinate, breaking up the description of relative motion into a distance and relative orientation measure. To avoid the singularity issues associated with a spherical coordinate description, an alternate method is proposed that uses the unit vector pointing from the chief to the deputy, as illustrated in Fig. 2. This unit vector is defined as

$$\hat{\boldsymbol{e}} = \frac{\boldsymbol{\rho}}{\rho} \tag{4}$$

To fully describe the relative position, a position coordinate along this unit vector is needed. This position coordinate is denoted as L. Using this description, the position of the deputy with respect to the chief in Hill-frame components is given by

$$\boldsymbol{\rho} = Le_1\hat{o}_r + Le_2\hat{o}_\theta + Le_3\hat{o}_h \tag{5}$$

where e_i are the Hill-frame components of $\hat{e}$. The forward and inverse mapping between the Cartesian Hill-frame components and the unit-vector description is given by

$$\begin{bmatrix} x \\ y \\ z \end{bmatrix} = \begin{bmatrix} Le_1 \\ Le_2 \\ Le_3 \end{bmatrix}, \qquad \begin{bmatrix} e_1 \\ e_2 \\ e_3 \end{bmatrix} = \begin{bmatrix} x/L \\ y/L \\ z/L \end{bmatrix} \tag{6}$$

with $L^2 = x^2 + y^2 + z^2$. The conversion between the rates is given by

$$\begin{bmatrix} \dot{x} \\ \dot{y} \\ \dot{z} \end{bmatrix} = \begin{bmatrix} \dot{L}e_1 + L\dot{e}_1 \\ \dot{L}e_2 + L\dot{e}_2 \\ \dot{L}e_3 + L\dot{e}_3 \end{bmatrix}, \qquad \begin{bmatrix} \dot{e}_1 \\ \dot{e}_2 \\ \dot{e}_3 \end{bmatrix} = \begin{bmatrix} (\dot{x} - \dot{L}e_1)/L \\ (\dot{y} - \dot{L}e_2)/L \\ (\dot{z} - \dot{L}e_3)/L \end{bmatrix} \tag{7}$$

with the position-coordinate rate determined as $\dot{L} = (x\dot{x} + y\dot{y} + z\dot{z})/L$.

Considering the relationship between the Cartesian Hill-frame coordinates and the unit-vector description, an apparent singularity occurs at $L = 0$. This singularity is a result of the nonuniqueness of the unit vector at this separation distance. In fact, when the separation distance is zero, any arbitrary unit vector will appropriately convert the unit-vector description into the Cartesian coordinates. While this presents an issue mathematically, it is of little practical concern because a separation distance of zero is impossible with the actual craft. The unit-vector description is well defined everywhere else, and is thus a good candidate for describing arbitrary relative motion.

With the unit-vector description, four parameters are used to describe a three-dimensional location. Similar to the use of the four-dimensional Euler parameter (EP) set to describe a three-dimensional attitude, there must be a constraint on the parameters. In this case, the unity constraint

$$e_1^2 + e_2^2 + e_3^2 = 1 \tag{8}$$

must be satisfied at all times. Differentiating this constraint twice with respect to time yields

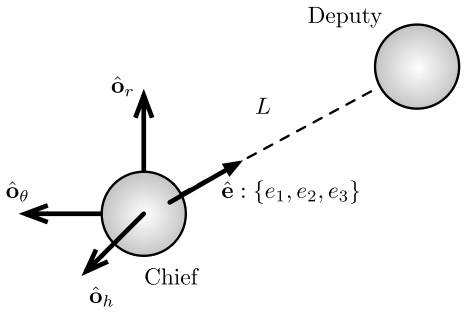

Fig. 2 Unit-vector description of relative motion.

$$e_1\ddot{e}_1 + e_2\ddot{e}_2 + e_3\ddot{e}_3 + \dot{e}_1^2 + \dot{e}_2^2 + \dot{e}_3^2 = 0 \tag{9}$$

Another parallel with the Euler parameter attitude description is the issue of uniqueness. When the four-dimensional Euler parameters are used to describe attitude, there are two sets that describe the same orientation. With the unit-vector relative motion description, there are two sets of parameters that describe the exact same relative position. In addition to the $\boldsymbol{\rho} = L\hat{e}$ description detailed previously, the same location may be obtained using $\boldsymbol{\rho} = -L(-\hat{e})$. This nonuniqueness has an important implication for the $\boldsymbol{\sigma}$ set introduced later in the paper.

To determine the relative equations of motion, Eqs. (6) and (7) are substituted into Eq. (3), and the constraint in Eq. (9) is used to yield

$$\begin{bmatrix} \ddot{L} \\ \ddot{e}_1 \\ \ddot{e}_2 \\ \ddot{e}_3 \end{bmatrix} = [f(L, \dot{L}, \hat{e}, \dot{\hat{e}})] + [G_e]\boldsymbol{u} \tag{10}$$

where

$$[f(L, \dot{L}, \hat{e}, \dot{\hat{e}})] = \begin{bmatrix} L(2n(e_1\dot{e}_2 - e_2\dot{e}_1) + n^2(3e_1^2 - e_3^2) + \dot{e}_1^2 + \dot{e}_2^2 + \dot{e}_3^2) \\ e_1(2ne_2\dot{e}_1 + n^2(3e_2^2 + 4e_3^2) - \dot{e}_1^2 - \dot{e}_2^2 - \dot{e}_3^2) - 2ne_1^2\dot{e}_2 + 2n\dot{e}_2 + 2\frac{\dot{L}}{L}(ne_2 - \dot{e}_1) \\ e_2(2n(e_2\dot{e}_1 - e_1\dot{e}_2) + n^2(e_3^2 - 3e_1^2) - \dot{e}_1^2 - \dot{e}_2^2 - \dot{e}_3^2) - 2n\dot{e}_1 - 2\frac{\dot{L}}{L}(ne_1 + \dot{e}_2) \\ -e_3((\dot{e}_1 - ne_2)^2 + 2ne_1\dot{e}_2 + 4n^2e_1^2 + \dot{e}_2^2 + \dot{e}_3^2) - 2\dot{e}_3\frac{\dot{L}}{L} \end{bmatrix} \tag{11a}$$

$$[G_e] = \frac{1}{L}\begin{bmatrix} Le_1 & Le_2 & Le_3 \\ 1 - e_1^2 & -e_1e_2 & -e_1e_3 \\ -e_1e_2 & 1 - e_2^2 & -e_2e_3 \\ -e_1e_3 & -e_2e_3 & 1 - e_3^2 \end{bmatrix} = \begin{bmatrix} \hat{e}^T \\ \frac{1}{L}([I] - \hat{e}\hat{e}^T) \end{bmatrix} \tag{11b}$$

$$u = \begin{bmatrix} u_x \\ u_y \\ u_z \end{bmatrix} \tag{11c}$$

Note that the only singularity in Eq. (10) occurs when $L = 0$. For reasons discussed previously, this is of little concern for the scope of this study. The unit-vector description provides practically nonsingular equations of motion that use the separation distance and a redundant set of orientation parameters to describe relative motion. In this manner, the singular issues that plague the spherical frame description are avoided while still maintaining a direct measure of the distance between the deputy and chief.

C. σ-Set Relative Motion Description

Now, an additional relative motion description is considered that is inspired by modified Rodrigues parameters (MRPs) [15]. The $\boldsymbol{\sigma}$ set contains L, the position coordinate along the unit vector, and two orientation parameters defined as

$$\boldsymbol{\sigma} = \begin{bmatrix} \sigma_1 \\ \sigma_2 \end{bmatrix} = \frac{1}{1 + e_1}\begin{bmatrix} e_2 \\ e_3 \end{bmatrix} = \frac{1}{x + L}\begin{bmatrix} y \\ z \end{bmatrix} \tag{12}$$

with the corresponding velocity mapping

$$\begin{bmatrix} \dot{\sigma}_1 \\ \dot{\sigma}_2 \end{bmatrix} = \frac{1}{x + L}\begin{bmatrix} \dot{y} \\ \dot{z} \end{bmatrix} - \frac{\dot{x} + \dot{L}}{(x + L)^2}\begin{bmatrix} y \\ z \end{bmatrix} \tag{13}$$

The inverse mapping between the $\boldsymbol{\sigma}$-set and Hill-frame coordinates is determined to be

$$\begin{bmatrix} x \\ y \\ z \end{bmatrix} = \frac{L}{1 + \sigma^2}\begin{bmatrix} 1 - \sigma^2 \\ 2\sigma_1 \\ 2\sigma_2 \end{bmatrix} \tag{14}$$

where $\sigma^2 = \sigma_1^2 + \sigma_2^2$. Taking the derivative with respect to time yields the velocity mapping

$$\begin{bmatrix} \dot{x} \\ \dot{y} \\ \dot{z} \end{bmatrix} = \frac{\dot{L}}{1 + \sigma^2}\begin{bmatrix} 1 - \sigma^2 \\ 2\sigma_1 \\ 2\sigma_2 \end{bmatrix} + \frac{2L}{(1 + \sigma^2)^2}\begin{bmatrix} -2\dot{\sigma}^T\sigma \\ (1 - \sigma_1^2 + \sigma_2^2)\dot{\sigma}_1 - 2\sigma_1\sigma_2\dot{\sigma}_2 \\ (1 + \sigma_1^2 - \sigma_2^2)\dot{\sigma}_2 - 2\sigma_1\sigma_2\dot{\sigma}_1 \end{bmatrix} \tag{15}$$

The relationship between the unit-vector and $\boldsymbol{\sigma}$-set parameters is presented in more detail in [16]. To obtain the equations of motion for the $\boldsymbol{\sigma}$ set, the previous relationships are inserted into the CW equations. The result is expressed in the form

$$\begin{bmatrix} \ddot{L} \\ \ddot{\sigma} \end{bmatrix} = [h(L, \dot{L}, \boldsymbol{\sigma}, \dot{\boldsymbol{\sigma}})] + [G_\sigma]\boldsymbol{u} \tag{16}$$

The three components of the $[h]$ matrix are

$$h_L = \frac{L}{(1 + \sigma^2)^2}[3n^2(\sigma_1^4 + \sigma_2^4 + 1) + 4\dot{\sigma}_1 n - 2n\sigma_2^2(5n + 2\dot{\sigma}_1) + 2n\sigma_1^2(3n(-1 + \sigma_2^2) + 2\dot{\sigma}_1) + 8n\sigma_1\sigma_2\dot{\sigma}_2 + 4\dot{\boldsymbol{\sigma}}^T\dot{\boldsymbol{\sigma}}] \tag{17a}$$

$$h_{\sigma_1} = -\frac{1}{2L(1 + \sigma^2)}[-6n^2L\sigma_1^3 + 2n\sigma_1^4\dot{L} + 4\sigma_1^2\dot{L}(n + \dot{\sigma}_1) - (1 + \sigma_2^2)\dot{L}(2n\sigma_2^2 - 2(n + 2\dot{\sigma}_1)) - 8L\sigma_2(n + \dot{\sigma}_1)\dot{\sigma}_2 + 2L\sigma_1(3n^2 - 5n^2\sigma_2^2 - 2\dot{\sigma}_1^2 + 2\dot{\sigma}_2^2)] \tag{17b}$$

$$h_{\sigma_2} = \frac{1}{2L(1 + \sigma^2)}[-4n\sigma_1^3\sigma_2\dot{L} - 4n\sigma_1(\sigma_2 + \sigma_2^3)\dot{L} - 4\dot{L}\dot{\sigma}_2 + 8L\sigma_1\dot{\sigma}_1\dot{\sigma}_2 + 2\sigma_1^2(2n^2L\sigma_2 - 2\dot{L}\dot{\sigma}_2) - \sigma_2(4\sigma_2\dot{L}\dot{\sigma}_2 + 4L(2n^2(1 - \sigma_2^2) + 2n\dot{\sigma}_1 + \dot{\sigma}_1^2 - \dot{\sigma}_2^2))] \tag{17c}$$

and the control sensitivity matrix is

$$[G_\sigma] = \begin{bmatrix} \frac{1 - \sigma^2}{1 + \sigma^2} & \frac{2\sigma_1}{1 + \sigma^2} & \frac{2\sigma_2}{1 + \sigma^2} \\ -\frac{\sigma_1}{L} & \frac{1 - \sigma_1^2 + \sigma_2^2}{2L} & -\frac{\sigma_1\sigma_2}{L} \\ -\frac{\sigma_2}{L} & -\frac{\sigma_1\sigma_2}{L} & \frac{1 + \sigma_1^2 - \sigma_2^2}{2L} \end{bmatrix} \tag{18}$$

The control vector $\boldsymbol{u}$ is defined the same as before, with components in the Hill frame. An examination of the $\boldsymbol{\sigma}$-set equations reveals singularities in two different positions. One occurs when $L = 0$, which corresponds to a collision between the chief and deputy. As

discussed previously, this is of little practical importance. The second singularity occurs when $x = -L$ (or $e_1 = -1$). This singularity must be given attention, as there are many possible trajectories that may encounter this configuration.

D. σ Shadow Set

As with the unit-vector description, there are two sets of L and $\boldsymbol{\sigma}$ values that describe the same relative position. This phenomenon is similar to the existence of a shadow set in the modified Rodrigues parameter attitude description [15]. Using the alternate unit-vector description $(-L, -\hat{e})$, the alternate $\boldsymbol{\sigma}$ set may be found. This shadow set, denoted as $\boldsymbol{\sigma}_s$, is defined as

$$\boldsymbol{\sigma}_s = -\frac{\boldsymbol{\sigma}}{\sigma^2} \tag{19}$$

Differentiating yields the shadow set velocity

$$\dot{\boldsymbol{\sigma}}_s = -\frac{\dot{\boldsymbol{\sigma}}}{\sigma^2} + 2\frac{\boldsymbol{\sigma}^T\dot{\boldsymbol{\sigma}}}{\sigma^4}\boldsymbol{\sigma} \tag{20}$$

where $\sigma^4 = (\sigma_1^2 + \sigma_2^2)^2$. For any relative motion, a set of $-L, -\dot{L}, \boldsymbol{\sigma}_s$, and $\dot{\boldsymbol{\sigma}}_s$ describes the exact same relative position and velocity as $L, \dot{L}$, $\boldsymbol{\sigma}$, and $\dot{\boldsymbol{\sigma}}$. In fact, one may switch between the original and shadow sets arbitrarily. Each set evolves according to the same differential equations.

This has important implications regarding the singularity at $x = -L$. If this singularity is approaching, a switch to the shadow set may be used to avoid it. When the original set is at the singularity, the shadow set is well defined at $\boldsymbol{\sigma} = 0$. By choosing an appropriate switching location, the arbitrary relative motion may be described using the $\boldsymbol{\sigma}$ set without encountering any singularities. Here, a switching condition of $\sigma^2 = 1$ is used. That is, when the magnitude of $\boldsymbol{\sigma}$ becomes larger than 1, a switch to the shadow set is employed. Considering the relationship between the unit-vector description and $\boldsymbol{\sigma}$ set, switching at this location restricts e_1 to only positive values, i.e., $e_1 \geq 0$. If $|\boldsymbol{\sigma}| \leq 1$, as is guaranteed by this switching condition, then e_1 is restricted to positive values due to the relationship $e_1 = (1 - \sigma^2)/(1 + \sigma^2)$. Changing back and forth between the original and shadow sets is equivalent to switching between $L, \hat{e}$ and $-L, -\hat{e}$.

III. Relative Motion Control

In this section, relative motion control is considered, using both the unit-vector description and σ set. The goal is tracking an arbitrary deputy trajectory. Because the CW equations are used to derive the equations of motion for these descriptions, only trajectories with a chief–deputy separation distance of less than 1 km are considered. It is assumed that the necessary control acceleration u is achievable by inertial thrusters.

A. Unit-Vector Control

The most apparent obstacle present when using the unit-vector description for control is the fact that there are only three control inputs for a four-dimensional system. However, the unit-vector components are not independent. Thus, it is possible to formulate the control problem in such a way as to obtain the desired tracking behavior using the three control inputs.

1. *Hill-Frame-Like Control*

For the first control law approach, consider the vector $\boldsymbol{R}$ defined as

$$\boldsymbol{R} = L\hat{e} \tag{21}$$

with the associated derivatives

$$\dot{\boldsymbol{R}} = \dot{L}\,\hat{e} + L\dot{\hat{e}} \tag{22a}$$

$$\ddot{\boldsymbol{R}} = \ddot{L}\,\hat{e} + 2\dot{L}\,\dot{\hat{e}} + L\ddot{\hat{e}} \tag{22b}$$

Note that the components of $\boldsymbol{R}$ are equivalent to the Cartesian Hill-frame components x, y, and z. Any set of L and $\hat{e}$ will describe exactly one $\boldsymbol{R}$ vector. Thus, if the system tracks a desired L and $\hat{e}$, then it will also track the equivalent $\boldsymbol{R}$. We may enforce tracking of L and $\hat{e}$, then, by tracking the $\boldsymbol{R}_r$ vector, defined as

$$\boldsymbol{R}_r = L_r\hat{e}_r \tag{23}$$

where L_r and $\hat{e}_r$ describe a desired reference trajectory. For the control law development, consider the candidate Lyapunov function [17]

$$V_1(\delta\boldsymbol{R}, \delta\dot{\boldsymbol{R}}) = \frac{1}{2}\delta\boldsymbol{R}^T[K]\delta\boldsymbol{R} + \frac{1}{2}\delta\dot{\boldsymbol{R}}^T\delta\dot{\boldsymbol{R}} \tag{24}$$

where $\delta\boldsymbol{R} = \boldsymbol{R} - \boldsymbol{R}_r$ and $[K]$ is a positive definite gain matrix. Geometrically, the tracking error $\delta\boldsymbol{R}$ is the vector from the reference position to the actual position of the deputy, as illustrated in Fig. 3. It makes sense, then, that driving this vector to 0 would lead to the tracking of the reference trajectory. The derivative of the candidate Lyapunov function with respect to time is

$$\dot{V}_1(\delta\boldsymbol{R}, \delta\dot{\boldsymbol{R}}) = \delta\dot{\boldsymbol{R}}^T([K]\delta\boldsymbol{R} + \ddot{\boldsymbol{R}} - \ddot{\boldsymbol{R}}_r) \tag{25}$$

For the deputy motion, the acceleration of $\boldsymbol{R}$ is

$$\ddot{\boldsymbol{R}} = [f_R] + \boldsymbol{u} = \begin{bmatrix} 2n(\dot{L}e_2 + L\dot{e}_2) + 3n^2Le_1 \\ -2n(\dot{L}e_1 + L\dot{e}_1) \\ -n^2Le_3 \end{bmatrix} + \begin{bmatrix} u_x \\ u_y \\ u_z \end{bmatrix} \tag{26}$$

Substituting this back into the Lyapunov rate function yields

$$\dot{V}_1(\delta\boldsymbol{R}, \delta\dot{\boldsymbol{R}}) = \delta\dot{\boldsymbol{R}}^T([K]\delta\boldsymbol{R} + [f_R] + \boldsymbol{u} - \ddot{\boldsymbol{R}}_r) \tag{27}$$

To ensure Lyapunov stability, the control law is chosen as

$$u = -[K]\delta\boldsymbol{R} - [P]\delta\dot{\boldsymbol{R}} + \ddot{\boldsymbol{R}}_r - [f_R] \tag{28}$$

where $[P]$ is a positive definite gain matrix. This control law results in the negative semidefinite Lyapunov rate

$$\dot{V}_1(\delta\boldsymbol{R}, \delta\dot{\boldsymbol{R}}) = -\delta\dot{\boldsymbol{R}}^T[P]\delta\dot{\boldsymbol{R}} \tag{29}$$

and closed-loop tracking dynamics

$$\delta\ddot{\boldsymbol{R}} + [P]\delta\dot{\boldsymbol{R}} + [K]\delta\boldsymbol{R} = 0 \tag{30}$$

To examine asymptotic stability, higher-order derivatives are taken and evaluated on the set $\delta\dot{\boldsymbol{R}} = 0$ [18]. The first nonzero derivative is found to be

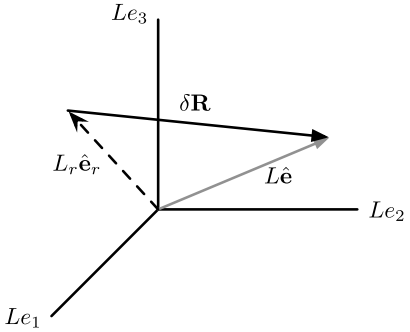

Fig. 3 The tracking error measure $\delta\boldsymbol{R}$ is the vector from the reference location to the current deputy position.

$$V_1(\delta\boldsymbol{R}, \delta\dot{\boldsymbol{R}} = 0) = -2\delta\boldsymbol{R}^T[K]^T[P][K]\delta\boldsymbol{R} \tag{31}$$

which is negative definite in terms of $\delta\boldsymbol{R}$. Thus, the control law tracks the reference trajectory asymptotically. Furthermore, the asymptotic stability is global, due to the radially unbounded nature of the candidate Lyapunov function in Eq. (24).

The control law in Eq. (28) does not linearize the dynamics of L and $\hat{e}$. Rather, it provides linear closed-loop tracking error dynamics. Using the unit-vector description, the preceding control law development provides a means to track an arbitrary, potentially time-varying reference trajectory. Its major drawback, however, is that it does not isolate the actuation of the separation distance from the relative orientation. For collision avoidance applications, it would be useful to be able to stabilize the relative separation distance more rapidly than relative orientation. This would allow for reorientation maneuvers that occur at a safely maintained separation distance. Indeed, one may argue that little is gained using this control law vs a similar development using Cartesian Hill-frame coordinates. After all, this control law is essentially actuating on these Hill-frame coordinates directly, albeit with a different description. While perhaps not ideal, these developments illustrate that it is possible to track an arbitrary reference trajectory using the unit-vector description.

2. *Isolating L and ê: γ Control Law*

For the next control development, the problem of isolating the separation distance actuation capabilities from the relative orientation is considered. That is, a control law is sought that would allow for tracking of some reference L_r more quickly than a reference orientation $\hat{e}_r$. Such a control would stabilize the relative separation distance early on in the maneuver before a large reorientation has occurred, thus minimizing the chance of collision. Rather than attempting to control all states of the system, only the separation distance and two elements of the unit vector are considered. As an example, consider an orientation error measure defined by e_1 and e_2. If the control is tracking a reference e_{1r} and e_{2r}, then

$$e_1^2 + e_2^2 + e_3^2 = 1 = e_{1r}^2 + e_{2r}^2 + e_{3r}^2 \tag{32}$$

Because $e_1 = e_{1r}$ and $e_2 = e_{2r}$, once the system has converged to the reference, it is guaranteed that

$$e_3 \to \pm e_{3r} \tag{33}$$

Thus, the system may converge to a state that is at the proper separation distance but not at the proper orientation. A similar argument may be repeated for any of the other pairs of unit-vector components. Determination of the conditions required for the convergence to the proper value is left for future work.

To arrive at a control law that isolates the separation distance from the relative orientation, consider the error measure $\delta\boldsymbol{\gamma}$, defined as

$$\delta\boldsymbol{\gamma} = \boldsymbol{\gamma} - \boldsymbol{\gamma}_r = \begin{bmatrix} L \\ e_i \\ e_j \end{bmatrix} - \begin{bmatrix} L_r \\ e_{ir} \\ e_{jr} \end{bmatrix} \tag{34}$$

where e_i and e_j denote any two components of $\hat{e}$. This error measure is used to define the candidate Lyapunov function

$$V_2(\delta\boldsymbol{\gamma}, \delta\dot{\boldsymbol{\gamma}}) = \frac{1}{2}\delta\boldsymbol{\gamma}^T[K]\boldsymbol{\gamma} + \frac{1}{2}\delta\dot{\boldsymbol{\gamma}}^T\delta\dot{\boldsymbol{\gamma}} \tag{35}$$

where $[K]$ is a positive definite gain matrix. The derivative of this Lyapunov function is

$$\dot{V}_2(\delta\boldsymbol{\gamma}, \delta\dot{\boldsymbol{\gamma}}) = \delta\dot{\boldsymbol{\gamma}}^T([K]\delta\boldsymbol{\gamma} + \ddot{\boldsymbol{\gamma}} - \ddot{\boldsymbol{\gamma}}_r) \tag{36}$$

The differential equation for $\boldsymbol{\gamma}$ is

$$\ddot{\boldsymbol{\gamma}} = [f_\gamma] + [G_\gamma]\boldsymbol{u} \tag{37}$$

where the elements of $[f_\gamma]$ and $[G_\gamma]$ are populated from Eq. (10), depending on which components of $\hat{\boldsymbol{e}}$ are used. Substituting these dynamics back into the Lyapunov rate expression yields

$$\dot{V}_2(\delta\boldsymbol{\gamma}, \delta\dot{\boldsymbol{\gamma}}) = \delta\dot{\boldsymbol{\gamma}}^T([K]\delta\boldsymbol{\gamma} + [f_\gamma] + [G_\gamma]\boldsymbol{u} - \ddot{\boldsymbol{\gamma}}_r) \tag{38}$$

To ensure stability, the control requirement used for the system is

$$[G_\gamma]\boldsymbol{u} = -[f_\gamma] - [K]\delta\boldsymbol{\gamma} - [P]\delta\dot{\boldsymbol{\gamma}} + \ddot{\boldsymbol{\gamma}}_r \tag{39}$$

where $[P]$ is a positive definite gain matrix. This results in the negative semidefinite Lyapunov rate:

$$\dot{V}_2(\delta\boldsymbol{\gamma}, \delta\dot{\boldsymbol{\gamma}}) = -\delta\dot{\boldsymbol{\gamma}}^T[P]\delta\dot{\boldsymbol{\gamma}} \tag{40}$$

As before, asymptotic stability is determined through the consideration of higher-order derivatives of V_2 [18]. Evaluated on the set $\delta\dot{\boldsymbol{\gamma}} = 0$, the first nonzero derivative is

$$\dddot{V}_2(\delta\boldsymbol{\gamma}, \delta\dot{\boldsymbol{\gamma}} = 0) = -2\delta\boldsymbol{\gamma}^T[K]^T[P][K]\delta\boldsymbol{\gamma} \tag{41}$$

which is negative definite in terms of $\delta\boldsymbol{\gamma}$. Thus, if Eq. (39) is satisfied, the system is asymptotically stable. The region of stability is global, due to the radially unbounded nature of V_2.

To find the control acceleration, $[G_\gamma]$ must be inverted and multiplied by the right-hand side of Eq. (39). This presents a problem, however, as $[G_\gamma]$ is not always invertible. The nature of this singularity becomes evident when considering the determinant of $[G_\gamma]$. It is solely a function of L and e_k,

$$|[G_\gamma]| = \frac{e_k}{L^2} \tag{42}$$

where e_k is the component of $\hat{e}$ not used in $\boldsymbol{\gamma}$. If the relative motion is desired in the chief orbit plane, for example, e_1 and e_2 cannot be used in $\boldsymbol{\gamma}$, or $[G_\gamma]$ will be singular all along the reference trajectory, where $e_3 = 0$.

The singularity issue is a very significant drawback to using this second control law to track a reference trajectory. If e_1 and e_2 are used in $\boldsymbol{\gamma}$, any trajectory that crosses from one side of the chief orbital plane to the other will encounter a singularity at the moment of crossing. If e_2 and e_3 are used in $\boldsymbol{\gamma}$, a trajectory that moves from above to below the chief (or vice versa) will pass through the singularity. Lastly, if e_1 and e_3 are used in $\boldsymbol{\gamma}$, any trajectory that passes from in front to behind the chief (or vice versa) will encounter the singularity issues. These conditions are extremely limiting on the number of reference trajectories that may be followed, and the performance of the system is very dependent on the starting location of the deputy. If the deputy is able to reach and converge onto the reference trajectory before a singularity is encountered, then no problems will occur. However, for arbitrary reference motion and initial deputy conditions, this is unlikely to be the case.

Let us turn our attention to a specific example of converging onto a naturally occurring relative motion. It is well known that, for close separation distances, a naturally occurring relative motion is a 2×1 ellipse in the chief orbit plane. We will assume, at least for this example, that the ellipse is centered on the chief. It would not be possible to use e_1 and e_2 in $\boldsymbol{\gamma}$ for this case due to the fact that $e_3 = 0$ all along the reference trajectory. Thus, it would be required to use e_3 and either e_1 or e_2 in $\boldsymbol{\gamma}$. However, both e_1 and e_2 will pass through 0 twice during each revolution of the ellipse. This example illustrates how significant the singularity issues are, even in enforcing simple, naturally occurring motion.

The second major issue is the indeterminacy of e_k. There is no guarantee that the relative orientation will converge to the reference. It is likely that, if the deputy starts closer to e_{kr} than $-e_{kr}$, it will converge to the proper orientation, but there is no guarantee. Furthermore, note that, to converge from a position near e_{kr} onto $-e_{kr}$, the system would have to pass through the singularity. For example, assume that e_3 is not used in γ. If e_{3r} is a positive value, and

$e_3(t_0)$ is also positive, the only way the system could converge to $-e_{3_r}$ is if e_3 passed through the singularity at 0.

B. σ-Set Control

The σ set is a minimal description. That is, three parameters are used to describe motion in a three-dimensional system. The problem of overdetermination that affected the unit-vector control law development is not an issue here. To develop a $\boldsymbol{\sigma}$-based control law, the error parameter $\delta\boldsymbol{\zeta}$ is used, where

$$\delta\boldsymbol{\zeta} = \boldsymbol{\zeta} - \boldsymbol{\zeta}_r = \begin{bmatrix} L \\ \boldsymbol{\sigma} \end{bmatrix} - \begin{bmatrix} L_r \\ \boldsymbol{\sigma}_r \end{bmatrix} \tag{43}$$

Consider the candidate Lyapunov function

$$V_3(\delta\boldsymbol{\zeta}, \delta\dot{\boldsymbol{\zeta}}) = \frac{1}{2}\delta\boldsymbol{\zeta}^T[K]\delta\boldsymbol{\zeta} + \frac{1}{2}\delta\dot{\boldsymbol{\zeta}}^T\delta\dot{\boldsymbol{\zeta}} \tag{44}$$

where $[K]$ is a positive definite gain matrix. The derivative of this Lyapunov function is

$$\dot{V}_3(\delta\boldsymbol{\zeta}, \delta\dot{\boldsymbol{\zeta}}) = \delta\dot{\boldsymbol{\zeta}}^T([K]\delta\boldsymbol{\zeta} + \ddot{\boldsymbol{\zeta}} - \ddot{\boldsymbol{\zeta}}_r)$$

Substituting in Eq. (16) yields

$$\dot{V}_3(\delta\boldsymbol{\zeta}, \delta\dot{\boldsymbol{\zeta}}) = \delta\dot{\boldsymbol{\zeta}}^T([K]\delta\boldsymbol{\zeta} + [h] + [G_\sigma]\boldsymbol{u} - \ddot{\boldsymbol{\zeta}}_r)$$

To ensure Lyapunov stability, the control law

$$\boldsymbol{u} = [G_\sigma]^{-1}(-[K]\delta\boldsymbol{\zeta} - [P]\delta\dot{\boldsymbol{\zeta}} - [h] + \ddot{\boldsymbol{\zeta}}_r) \tag{45}$$

is chosen, where $[P]$ is a positive definite gain matrix. This reduces the Lyapunov rate to

$$\dot{V}_3(\delta\boldsymbol{\zeta}, \delta\dot{\boldsymbol{\zeta}}) = -\delta\dot{\boldsymbol{\zeta}}^T[P]\delta\dot{\boldsymbol{\zeta}}$$

which is negative semidefinite. To determine asymptotic stability, higher-order derivatives of the Lyapunov function are taken and evaluated on the set $\delta\dot{\boldsymbol{\zeta}} = 0$ [18]. The first nonzero derivative is

$$\dddot{V}_3(\delta\boldsymbol{\zeta}, \delta\dot{\boldsymbol{\zeta}}) = -2\delta\boldsymbol{\zeta}^T[K]^T[P][K]\delta\boldsymbol{\zeta}$$

which is negative definite in terms of $\delta\boldsymbol{\zeta}$. Thus, the control law tracks the reference trajectory asymptotically.

The act of switching between the original and shadow sets has important implications for the control response. The preceding Lyapunov stability analysis assumes that V_3 and its derivatives are continuous. Switching to the shadow set violates this continuity assumption. Furthermore, the signs of L and L_r may present problems. If $L < 0$ and $L_r > 0$, for instance, the control law will strive to move the deputy through $L = 0$ to positive values where it will track L_r. Not only is this a collisional hazard, but passing through $L = 0$ is a singularity for the $\boldsymbol{\sigma}$ set.

Each of these issues may be addressed by switching the reference trajectory to its shadow set so that the signs of L and L_r are always the same. If the deputy position description is switched from the original to the shadow set, then the reference trajectory must be switched as well. Consider two Lyapunov functions V_o and V_s, formed using the original and shadow $\boldsymbol{\sigma}$ sets. With the control law in Eq. (45) formulated as a function of the original $\boldsymbol{\sigma}$ set, the Lyapunov stability analysis guarantees that the system will converge toward the reference. Because the original and shadow $\boldsymbol{\sigma}$ sets describe the exact same relative positions, a convergence in one implies a convergence in the other. Thus, as V_o is decreasing, V_s must also be decreasing. When a switch is called for, the value of V_3 changes from V_o to V_s. In fact, at each switching time, the value of V_3 changes back and forth between these two continuously decreasing functions, as illustrated in Fig. 4. Thus, the system is still guaranteed to converge asymptotically in spite of the discontinuous switching.

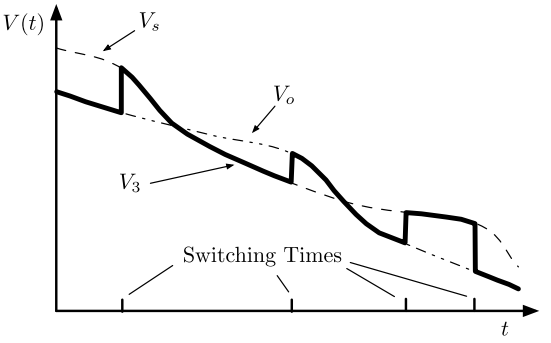

Fig. 4 The Lyapunov function V_3 switches between two continuously decreasing functions as σ is switched to the shadow set.

There is a potential issue with switching the reference trajectory to its shadow set. It is possible that the reference trajectory may be switched onto a singularity. Consider the following example. If the reference location is at $x = -50$ m in the Hill frame, the only defined $\boldsymbol{\sigma}$-set description for this position is $L = -50$ m, $\boldsymbol{\sigma} = 0$. If the deputy motion calls for the reference trajectory to switch to its shadow set, it will shift onto the singularity.

IV. Numerical Simulation

To validate and illustrate the performance of the unit-vector and $\boldsymbol{\sigma}$-set control laws, numerical simulation is used. Each of the control laws is implemented into an inertial simulation. For the inertial simulation, the trajectory of each craft is determined from the integration of

$$\ddot{\boldsymbol{r}}_i = -\frac{\mu}{r^3}\boldsymbol{r}_i + \boldsymbol{u} \tag{46}$$

where $\boldsymbol{u}$ is determined from the control laws developed earlier in this work. In this paper, continuous thrust is assumed. While this may not be a realistic assumption for actual thrusters, a realistic thruster implementation is beyond the scope of this research. In practice, pulse-width modulation on the thrusters would be a way to approximate a continuous thrust profile [19].

The relative motion is computed using the inertial trajectories of each craft. The initial conditions for each simulation are determined by defining a set of orbital elements for the chief and orbit element differences for the deputy. The values used for the simulations are summarized in Table 1. Because the unit-vector and $\boldsymbol{\sigma}$-set equations of motion are obtained from the linearized CW equations, the orbital element differences will be kept at small levels such that the linear approximation is valid.

A. Unit-Vector γ Control Law

To demonstrate the performance of the unit-vector γ control law, a time-varying reference trajectory is prescribed in the Hill frame, and the control law is applied to track the reference. The target reference motion, which is not a naturally occurring motion, is

$$x_r(t) = 0.05\ \cos(nt)(\text{km}) \tag{47a}$$

$$y_r(t) = 0.05\ \sin(nt)(\text{km}) \tag{47b}$$

$$z_r(t) = 0.02\ \sin(2nt + \pi/2) + 0.03(\text{km}) \tag{47c}$$

Table 1 Orbit elements for chief and deputy craft

	a, km	e	i, deg	Ω, deg	ω, deg	M_0, deg
Chief	7500	0	20	10	250	0
Deputy	$a_c + 0.05$	$e_c + 0.00001$	$i_c - 0.001$	Ω_c	$\omega_c + 0.0001$	$M_{0,c}$

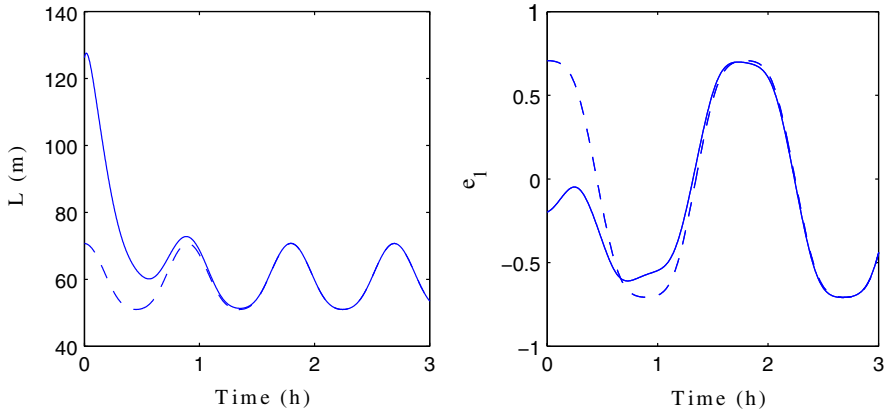

a) L History b) e_1 History

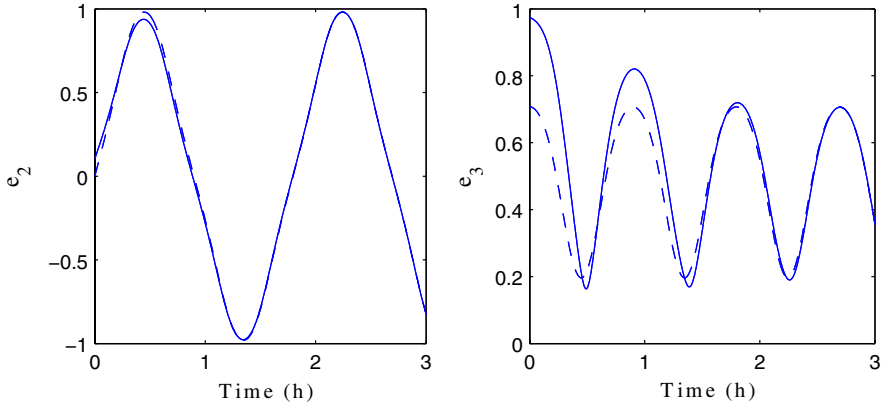

c) e_2 History d) e_3 History

Fig. 5 Time histories of L and $\hat{e}$ during the tracking maneuver. The reference trajectory is shown as a dashed line.

The z coordinate is maintained positive to avoid singularity issues that would occur for the case in which e_3 would pass from negative ($-z$) to positive ($+z$). The reference trajectory is transformed into unit-vector components for implementation into the control law, with gains of $[K] = n^2\text{diag}([10; 1; 1])$ and $[P] = n\text{diag}([10; 1; 1])$. Gain selection is important for this scenario. Improper gain selection will cause the system to encounter the singular transition from $+z$ to $-z$. Here, appropriate gains are chosen to avoid encountering the singularity and illustrate proper functionality of the control law.

The $\boldsymbol{\gamma}$ control law is applied using L, e_1, and e_2 for the error measure. By weighting the separation distance error 10 times higher than the relative orientation error, the singularity is avoided. The time histories of L and $\hat{e}$ during the maneuver are shown in Fig. 5, and the state errors are presented in Fig. 6. Because of the higher gains on the L error, the rate of convergence to the reference separation distance is faster than the rate of convergence to the reference orientation.

The control inputs generated by the γ control law are shown in Fig. 7. The transient response necessary for the deputy to reach the reference trajectory is evident, followed by the nonzero control required to maintain the nonnaturally occurring reference motion. The magnitude of control acceleration needed is on the order of millimeters per second squared.

B. σ-Set Control Law

A major advantage of the $\boldsymbol{\sigma}$-set description is that it isolates the separation distance from the relative orientation. Using proper gain selection, a desired separation distance may be achieved quickly and maintained during reorientation. For example, if the deputy is to be repositioned from ahead of to behind the chief, a safe separation distance may be maintained while the deputy moves around the chief. To illustrate this point, gains are chosen that cause the deputy to track

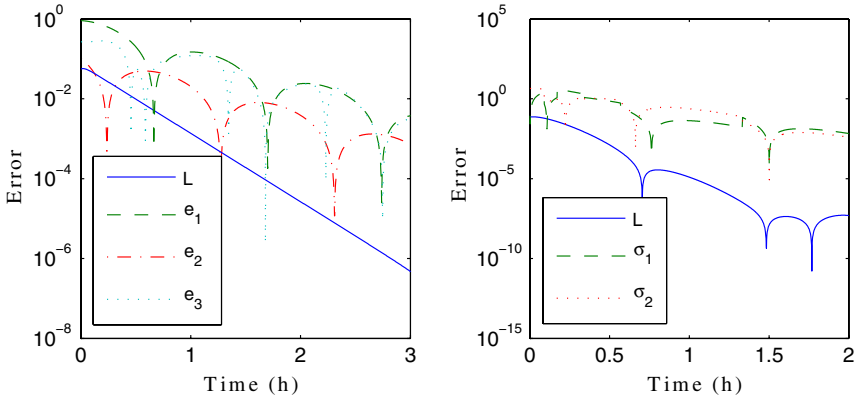

a) γ Control law b) σ-Set control law

Fig. 6 State errors for unit-vector and σ-set control laws throughout tracking maneuvers.

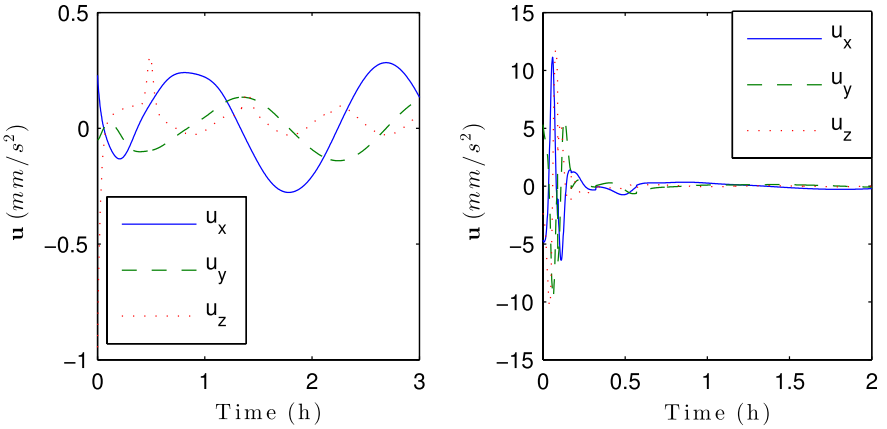

a) γ Control law **b) σ-Set control law**

Fig. 7 Control inputs for unit-vector γ control law and σ-set control law.

the reference separation distance L_r more quickly than the relative orientation $\boldsymbol{\sigma}$. The $\boldsymbol{\sigma}$-set control law developed previously effectively linearizes the closed-loop dynamics into the form

$$\delta\ddot{\boldsymbol{\zeta}} + [P]\delta\dot{\boldsymbol{\zeta}} + [K]\boldsymbol{\zeta} = 0$$

By choosing diagonal $[K]$ and $[P]$ gain matrices, the response of the system for L tracking is independent of $\boldsymbol{\sigma}$ tracking. Here, a slightly underdamped response is desired with a damping ratio of $\zeta = 0.925$. For this system, the desired gains for a given settling time, T_s, are computed as [5,20]

$$K_i = \frac{27.829}{T_s^2} \qquad P_i = 1.85\sqrt{K_i}$$

The settling time for L is chosen as 30 min, while the settling times for $\hat{e}$ and $\boldsymbol{\sigma}$ are chosen as 1 h.

To illustrate tracking performance, once again, a time-varying trajectory is specified in Hill-frame coordinates. The trajectory used is

$$x_r(t) = 0.05\ \cos(nt)(\text{km}) \tag{48a}$$

$$y_r(t) = 0.05\ \sin(nt)(\text{km}) \tag{48b}$$

$$z_r(t) = 0.02\ \sin(2nt + \pi/2)(\text{km}) \tag{48c}$$

During the simulation, the switching conditions of $|\boldsymbol{\sigma}| = 1$ are employed, and the reference trajectory is switched to its shadow set during every deputy switch so that $\text{sign}(L) = \text{sign}(L_r)$. The time histories of L and $\boldsymbol{\sigma}$ during the maneuver are shown in Fig. 8. The state errors over the same time period are shown in Fig. 6. The

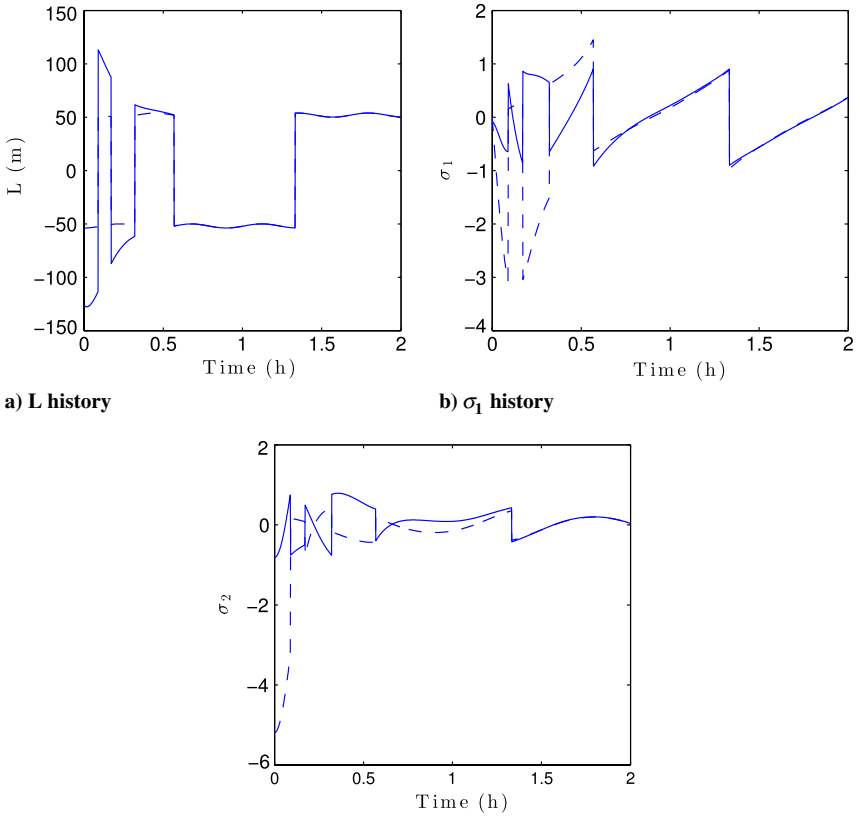

a) L history **b) σ_1 history**

c) σ_2 history

Fig. 8 Time histories of L and σ during the tracking maneuver. The reference trajectory is shown as a dashed line.

switching times are evident, both for the actual and reference trajectories. While the magnitude of $\boldsymbol{\sigma}$ is constrained to be less than 1, the magnitude of $\boldsymbol{\sigma}_r$ is not. The reason is due to the fact that $\boldsymbol{\sigma}_r$ is automatically switched to its shadow set when $|\boldsymbol{\sigma}|$ calls for it, regardless of whether or not $|\boldsymbol{\sigma}_r| \leq 1$.

The effects of gain selection on the system response are clear in Fig. 6. The separation distance has a rate of convergence to the reference that is twice as fast as the rate of convergence for $\boldsymbol{\sigma}$. The practical application for such a response is maintaining a safe separation distance during a reorientation maneuver. The control history for the $\boldsymbol{\sigma}$-set control law is shown in Fig. 7. Again, milimeters per second squared level control inputs are needed, and a nonzero control is required to track the reference trajectory.

V. Conclusions

Two new relative motion descriptions are developed that are inspired by attitude parameter sets. The unit-vector description and $\boldsymbol{\sigma}$ set both isolate the separation distance from relative orientation. Equations of motion using these new descriptions are derived from the well-known Clohessy–Wiltshire equations. Reference trajectory tracking control laws are developed and implemented in numeric simulation. The unit-vector description is nonsingular, and the $\boldsymbol{\sigma}$ set can avoid singularities by switching to its shadow set. However, the control laws developed for these descriptions may encounter unavoidable singularities. The issues present in the unit-vector γ control law are due to the fact that the description is overdetermined. That is, a four-dimensional system is actuated upon by a three-dimensional control vector. With the $\boldsymbol{\sigma}$ set, the control singularities are due to the fact that, when a switch to the shadow set is called for, the reference trajectory must be switched as well. Although the $\boldsymbol{\sigma}$ set is switched in such a way as to avoid singularities, the same cannot be said about the reference trajectory. Because the reference switching is dependent on the actual deputy trajectory, a switch may be called for that places the reference trajectory right on a singular orientation. Careful planning may be required to prevent issues from affecting control system performance. This remains an open question for future research.

References

[1] Clohessy, W. H., and Wiltshire, R. S., "Terminal Guidance System for Satellite Rendezvous," *Journal of the Aerospace Sciences*, Vol. 27, No. 9, 1960, pp. 653–658. doi:10.2514/8.8704

[2] De Bruijn, F. J., Gill, E., and How, J., "Comparative Analysis of Cartesian and Curvilinear Clohessy–Wiltshire Equations," *22nd International Symposium on Space Flight Dynamics*, Instituto Nacional de Pesquisas Espaciais, 2011.

[3] Jiang, F., Li, J., and Baoyin, H., "Approximate Analysis for Relative Motion of Satellite Formation Flying in Elliptical Orbits," *Celestial Mechanics and Dynamical Astronomy*, Vol. 98, No. 1, 2007, pp. 31–66. doi:10.1007/s10569-007-9067-8

[4] Condurache, D., and Martinusi, V., "Quaternionic Exact Solution to the Relative Orbital Motion Problem," *Journal of Guidance, Control, and Dynamics*, Vol. 33, No. 4, 2010, pp. 1035–1047. doi:10.2514/1.47782

[5] Hogan, E., and Schaub, H., "Relative Motion Control for Two-Spacecraft Electrostatic Orbit Corrections," *Journal of Guidance, Control, and Dynamics*, Vol. 36, No. 1, 2013, pp. 240–249. doi:10.2514/1.56118

[6] Schaub, H., and Moorer, D. F., "Geosynchronous Large Debris Reorbiter: Challengs and Prospects," *AAS Kyle T. Alfriend Astrodynamics Symposium*, Univelt, Inc., San Diego, CA, 2010.

[7] Schaub, H., and Jasper, L. E. Z., "Orbit Boosting Maneuvers for Two-Craft Coulomb Formations," *Journal of Guidance, Control, and Dynamics*, Vol. 36, No. 1, 2013, pp. 74–82. doi:10.2514/1.57479

[8] Bombardelli, C., and Pelaez, J., "Ion Beam Shepherd for Contactless Space Debris Removal," *Journal of Guidance, Control, and Dynamics*, Vol. 34, No. 3, 2011, pp. 916–920. doi:10.2514/1.51832

[9] Kitamura, S., "Large Space Debris Reorbiter using Ion Beam Irradiation," *61st International Astronautical Congress*, Curran Associates, Inc., Red Hook, NY, 2010.

[10] Bombardelli, C., Urrutxua, H., Merino, M., Ahedo, E., Pelaez, J., and Olympio, J., "Dynamics of Ion-Beam Propelled Space Debris," *International Symposium on Space Flight Dynamics*, Instituto Nacional de Pesquisas Espaciais, 2011.

[11] Wiener, T. F., "Theoretical Analysis of Gimballess Inertial Reference Equipment Using Delta-Modulated Instruments," Ph.D. Dissertation, Dept. of Aeronautics and Astronautics, Massachusetts Inst. of Technology, Cambridge, MA, March 1962.

[12] Marandi, S. R., and Modi, V. J., "A Preferred Coordinate System and the Associated Orientation Representation in Attitude Dynamics," *Acta Astronautica*, Vol. 15, No. 11, 1987, pp. 833–843. doi:10.1016/0094-5765(87)90038-5

[13] Tsiotras, P., "On the Choice of Coordinates for Control Problems on SO (3)," *30th Annual Conference on Information Sciences and Systems*, IEEE, 1996, pp. 1238–1243.

[14] Schaub, H., and Junkins, J. L., "Stereographic Orientation Parameters for Attitude Dynamics: A Generalization of the Rodrigues Parameters," *Journal of Astronautical Sciences*, Vol. 44, No. 1, 1996, pp. 1–19.

[15] Schaub, H., and Junkins, J. L., *Analytical Mechanics of Space Systems*, AIAA Education Series, 2nd ed., AIAA, Reston, VA, 2009, pp. 117–125.

[16] Hogan, E. A., and Schaub, H., "Attitude Parameter Inspired Descriptions of Relative Orbital Motion," *AIAA/AAS Astrodynamics Specialist Conference*, AIAA Paper 2012-4739, 2012.

[17] Schaub, H., Vadali, S. R., and Alfriend, K. T., "Spacecraft Formation Flying Control Using Mean Orbit Elements," *Journal of Astronautical Sciences*, Vol. 48, No. 1, 2000, pp. 69–87.

[18] Mukherjee, R., and Chen, D., "Asymptotic Stability Theorem for Autonomous Systems," *Journal of Guidance, Control, and Dynamics*, Vol. 16, No. 5, 1993, pp. 961–963. doi:10.2514/3.21108

[19] Agrawal, B. N., Mcclelland, R., and Song, G., "Attitude Control of Flexible Spacecraft Using Pulse-Width Pulse-Frequency Modulated Thrusters," *Space Technology*, Vol. 17, No. 1, 1997, pp. 15–34.

[20] Nise, N. S., *Control Systems Engineering*, 5th ed., Wiley, Hoboken, NJ, 2008, pp. 170–174.